ENVIRONMENTAL TECHNOLOGY, 2017
VOL. 38, NO. 22, 2811–2823
http://dx.doi.org/10.1080/09593330.2016.1278462

Taylor & Francis
Taylor & Francis Group

Sorption studies of diethylketone in the presence of Al^{3+}, Cd^{2+}, Ni^{2+} and Mn^{2+}, from lab-scale to pilot scale

Filomena Costa and Teresa Tavares

Centre of Biological Engineering, University of Minho, Braga, Portugal

ABSTRACT

The toxic effects of diethylketone (DEK) in aqueous solution with different concentrations of Al^{3+}, Cd^{2+}, Ni^{2+} and Mn^{2+} were evaluated at lab-scale. It was established that *Streptococcus equisimilis* is able to efficiently remove DEK with different concentrations with heavy metals. It was proved that this joint-system has excellent capacity to biodegrade high concentrations of DEK in the presence of Al^{3+}, Cd^{2+}, Ni^{2+} and Mn^{2+}. With the exception of Al^{3+}, the uptake for all metals increased as the initial concentration of each metal in the mixed solution increased. The breakthrough curves are best described by the Adams and Bohart model for Cd^{2+}, by the Yoon and Nelson model for Ni^{2+} and by the Wolborska model for Mn^{2+}.

ARTICLE HISTORY
Received 5 August 2016
Accepted 28 December 2016

KEYWORDS
Breakthrough curves; diethylketone; heavy metals; kinetics; *Streptococcus equisimilis*

Introduction

One of the environment subjects of greatest importance and concern relates to the pollution of aquatic and terrestrial systems with heavy metals and volatile organic compounds (VOCs) and its consequences on life and ecology [1]. This is particularly problematic as, in addition to not being biodegradable, metals tend to accumulate in living organisms and in living tissues via food chain, triggering numerous diseases and health disorders [2]. Heavy metals can enhance and/or increase the toxic and inhibitory effects on the microbial growth. Heavy metals can enter the environment through aqueous effluents from different industries such as electronic devices manufacturing, oil refining, printing, dyes, paints, pulp and paper, fertilizers, pesticides, steels [1], jewelry, mining, tanneries, textile, batteries, petrochemical and fine chemistry, chemicals production and health-care products [3]. Toxic metals such as aluminum (Al^{3+}), cadmium (Cd^{2+}), nickel (Ni^{2+}) and manganese (Mn^{2+}) are among the most common metal pollutants present in soil and water [4]. Although toxic when present in high concentrations, metals such as nickel and manganese are required for the functioning of several cellular enzymes (co-factors, also known as essential metals or micro-nutrients) such as urease and hydrogenase, manganese superoxide dismutase, pyruvate carboxylase and for the activation of others enzymes such as kinases, decarboxylases, transferases and hydrolases. Ni release into the environment can occur from biogenic sources such as windblown, dust and volcanic eruptions. However, the majority of its release comes from the burning of residual and fuel oils from metal refining, municipal incineration, steel production and coal production [5]. Ni is considered a carcinogenic element, able to cause several kinds of acute and chronic health disorders such as skin dermatitis, chest pain, lungs and kidney damage, nausea, pulmonary fibrosis, renal edema, cyanosis and extreme weakness [6]. Manganese and manganese compounds are employed mainly in the manufacture of steel and iron alloys, batteries, glass and fireworks. They are also used as oxidants for cleaning, bleaching and disinfection purposes, livestock feeding supplements and in fertilizers, varnish and fungicides [7]. Exposure to manganese may occur either orally or by inhalation and can onset serious toxic responses. Usually, the initial symptoms are headache, disorientation, anxiety, insomnia, memory loss and lethargy. With continued exposure, these symptoms can develop and lead to motor disturbances, tremors and difficulty in walking. Aluminum and cadmium, on the other hand, do not present any biological activity or function (nonessential metals). Aluminum can be used in an extensive variety of industries (aircraft, automotive and construction, as a structural material), products (cooking utensils, food packaging, metal alloys, pigments, paints, heat resistant fibers, pharmaceutical and personal care products) and compounds (food additives, antacids, antiperspirants) [8]. Exposure to aluminum may affect particularly people with kidney disorders, since they have less capacity to remove this metal from their body. Although the health effects of aluminum on humans are not

CONTACT Filomena Costa filomenacpcosta@ceb.uminho.pt Centre of Biological Engineering, University of Minho, Campus de Gualtar, Braga 4710-057, Portugal

definitive and perceived, the Joint Food and Agriculture Organization and the World Health Organization Expert Committee on Food Additives lowered the allowable intake of aluminum in 2006, from 7 mg/kg body weight to 1 mg/kg body weight per week [9]. Cadmium is employed in six major classes: Ni–Cd batteries, cadmium pigments, cadmium stabilizers, cadmium coatings, cadmium alloys and cadmium electronic compounds such as cadmium telluride (CdTe) [10]. Exposure to cadmium may affect the action of enzymes, hampering respiration, photosynthesis, transpiration and chlorosis [11], cause cancer, lead to infertility and promote severe health problems in different organs. Cadmium presents also high mobility in soil, high solubility in water and extreme toxicity, even at low concentration [2].

VOCs such as ketones are usually released into the atmosphere by biogenic and anthropogenic sources. Diethylketone (DEK), also known as 3-pentanone, is a simple symmetrical dialkyl ketone that is naturally produced and released into nature by plants, fruits [12,13] and produced industrially to be used as solvent or polymer precursor [14], as an intermediate in the synthesis of pharmaceuticals, cosmetics, flavors and pesticides [15]. Besides reacting with OH radicals promoting the formation of ozone and other components of the photochemical smog in urban areas [14], DEK is persistent in water, soil and air and presents high mobility [16] and ability to form toxic and phototoxic intermediates [17]. Exposure to DEK may cause, according to the Occupational Safety and Health Hazards (OSHA) of United States Department Labor, skin and eyes irritation, coughing and sneezing. Prolonged exposure may cause shortness of breath, tachycardia, faintness, nausea, coma and even death. There are countless studies on heavy metal and organic solvents removal from wastewater. Techniques such as chemical precipitation, reverse osmosis, ion exchange, adsorption on granular activated carbon, condensation, thermal degradation, oxidation and incineration [18] present several disadvantages [19]. Studies conducted by numerous authors over the last few years have demonstrated that biological processes present several advantages over the traditional methods mentioned above. The biological processes present reduced maintenance and operation costs, high efficiency and eco-friendly character since they do not produce solid wastes and nitrogen oxides, which would require a secondary treatment [17,20].

Since some contaminated systems can contain simultaneously heavy metals and VOCs [3], the studies concerning the decontamination of this kind of systems and its subsequent optimization become of major importance and relevance not only for environment rehabilitation, but also aiming its economics sustainability.

In this study, a joint-system was used that combines the properties of clays and microorganisms to enhance the removal of different kind of pollutants from aqueous solutions. This joint-system combines the sorption capacity of the clay, providing excellent physical and chemical stability, large specific surface area, high cation exchange capacity [15] with the ability of the microorganisms to degrade, fix and/or entrap pollutants, due of the presence of several functional groups on the biomass surface [17]. The main goal of this work is the development of an environment-friendly technology able to treat multicomponent systems, containing DEK, aluminum, cadmium, nickel and manganese. Although these two types of pollutants (metals and ketones) appear together in the wastewater of different industries such as metal refining [21] and paint manufacturing [22], the knowledge regarding simultaneous treatment of water containing these pollutants is rather scarce.

The theoretical models used in the present work are described below.

Sorption kinetic models

The phenomena involved in biodegradation and/or biosorption processes are of utmost importance because they provide an understanding of the time dynamics of sorption processes and how they determine the chemical reaction, as well as the mass transfer and diffusion processes. These phenomena can differ significantly from open, semi-closed and closed systems, even when all the remaining conditions are kept equal. For a better understanding of DEK, Al^{3+}, Cd^{2+}, Ni^{2+} and Mn^{2+} removal kinetics by *Streptococcus equisimilis* (lab-scale experiments) and by *S. equisimilis* biofilm supported on vermiculite (pilot-scale experiments), the experimental results were fitted by the pseudo-first-order and pseudo-second models reported in the literature [23–25].

Breakthrough curves modeling

One of the prerequisites for a successful design of a fixed-bed column system for the removal of organic compounds and/or heavy metals in aqueous solution is the prediction of the concentration – time profile or breakthrough curve. In this study, the Adams-Bohart, Wolborska and Yoon and Nelson models were used to describe the breakthrough curves [26–30].

Experimental

Bacteria strain and vermiculite

Streptococcus equisimilis was obtained from the Spanish Type Culture Collection, at the University of Valencia,

with the following reference CECT 926. The vermiculite was purchased from Sigma-Aldrich and presents a Brunauer-Emmet and Teller surface area of 39 m^2/g, an average particle diameter of 8.45 mm and a porosity of 10%. In the present study, the bacterial biofilm was developed and established on the vermiculite.

Culture and chemicals properties

Streptococcus equisimilis was grown in sterilized Brain Heart Infusion (Oxoid CM1135) culture medium at 37°C, 150 rpm, for several days. DEK was purchased from Acros Organics (98% pure) and diluted in sterilized distilled water. Individual stock solutions of 1 g/L of aluminum ($Al(OH)_3$, Merck), 1 g/L of nickel ($NiCl_2{\cdot}6H_2O$, Carlo Erba Reagents), 1 g/L of cadmium ($CdSO_4{\cdot}8/3H_2O$, Riedel-de-Haën) and 1 g/L of manganese ($MnSO_4{\cdot}H_2O$, Panreac) were prepared by dissolving an accurately weighed amount of metal compound in sterilized distilled and deionized water. The multi-element inductively coupled plasma (ICP) quality control standard solution was purchased from CHEM Lab (QCS-03) (15E). The range of concentrations of each ion, Al^{3+}, Cd^{2+}, Ni^{2+} and Mn^{2+}, was obtained by dilution of the respective stock solution and varied between 5 and 100 mg/L.

Lab-scale experiments – biosorption in batch systems

Erlenmeyer flasks (1 L) containing 0.5 L of sterilized Brain Heart Infusion culture medium were inoculated with a pure culture of *S. equisimilis* and left to grow in an incubator for 24 h at 150 rpm and 37°C (Culture X). After this period, 250 mL of Culture X was transferred to 1 L of a new sterilized Brain Heart Infusion culture medium and left to grow on an incubator for 48 h at 150 rpm and 37°C (Culture Y). The lab-scale biosorption experiments were conducted in 0.250 L Erlenmeyer flasks containing 0.125 L of sterilized Brain Heart Infusion culture medium, 4 g/L of DEK and 5–100 mg/L of Al^{3+}, Cd^{2+}, Ni^{2+} and Mn^{2+}. These Erlenmeyer flasks were inoculated with 10 mL of the culture Y and incubated under orbital shaking (150 rpm) at 37°C for several days. At pre-establish times intervals samples were collected and centrifuged at 1300 rpm (Eppendorf MiniSpin 9056) for 10 min. The supernatant was analyzed by ICP-optical emission spectrometry (OES) and Gas chromatography-mass spectrometry (GC-MS) in order to quantify respectively the concentration of heavy metals and DEK. Two blanks were used. One containing only DEK and bacteria, and other containing 4 g/L of DEK and 5 mg/L of Al^{3+}, Cd^{2+}, Ni^{2+} and Mn^{2+}. The first blank was used to assess the growth of the bacteria, whereas the second blank assessed the eventual interaction between the different pollutants and the Erlenmeyer's walls. At the end of the experiments, samples were collected and inoculated in Petri dishes in order to confirm the metabolic activity of the bacteria. The pH along the assays was also monitored.

Pilot-scale experiments – biosorption in open systems

The pilot-scale experiments were conducted in a compact polycarbonate acrylic bioreactor of 22.7 L, with an internal diameter of 17 cm and a total height of 100 cm. One-third of the bioreactor was filled with vermiculite (700 g). For the biofilm development, a *S. equisimilis* culture was grown in an Erlenmeyer flask (2 L) containing 1 L of Brain Heart Infusion culture medium, previously sterilized at 121°C for 20 min. The Erlenmeyer flask was inoculated with *S. equisimilis*, incubated in orbital shaker for 24 h at 37°C and 150 rpm and capped with cotton stoppers in order to allow a passive aeration. The inoculum culture was transferred to the bioreactor setup and recirculated upwards at a flow rate of 250 mL/min during 5 days in order to allow the biomass to attach to the vermiculite and form a well-developed biofilm. Once the biofilm was formed, the bed was washed out and a 40 L solution containing 100 mg/L of each metal (Al^{3+}, Cd^{2+}, Ni^{2+} and Mn^{2+}) and 7.5 g/L of DEK (that acted as carbon source) was continuously pumped upwards through the bioreactor with a constant flow rate of 25 mL/min. Periodically, DEK was added to the working solution in order to continuously supply a carbon source to the biofilm and also to infer about its impact on the metals sorption. At pre-established time intervals, samples of the effluent were taken, centrifuged at 1300 rpm (Eppendorf MiniSpin 9056) for 10 min and the aqueous phase was analyzed by GC-MS and by ICP-OES in order to assess respectively the concentration of DEK and heavy metals through time. At the end, the bioreactor was washed out and samples of the effluent and of the vermiculite were inoculated in Petri dishes with Brain Heart Infusion culture medium, in order to confirm the metabolic activity of the bacteria. The pH was also measured.

Analytical methods

Gas chromatography

A GC-MS Varian 4000, equipped with a flame ionization detector, MS and a ZB-WAXplus column (30 m × 0.53 mm × 1.0 µm) was used to determine the

concentration of DEK in distinct samples. The column was initially held at a temperature 50°C, then heated at a rate of 3°C/min until it reached 100°C, then held at 100°C for 4 min, heated again at a rate of 40°C/min to 150°C and finally held at 150°C for 2 min. The temperature of the injector and detector were kept at 250°C. Nitrogen was used as the carrier gas at a flow rate of 4 mL/min and the injections were performed in the split mode with a split ratio of 1:10. The concentration of DEK was determined by comparing the areas of the peak of the internal standard (2-methyl-1-butanol) to the areas and retention time of the peaks appearing in the samples taken during the experiments. The retention time for DEK and for the internal standard was found to be respectively 5.3 and 11.3 min.

Inductively coupled plasma optical emission spectrometry

An ICP-OES (Optima 8000, PerkinElmer) was used to measure the concentration of Al^{3+}, Cd^{2+}, Ni^{2+} and Mn^{2+} through time for the lab and pilot-scale experiments. The operating conditions were as follows: 1300 W of radio frequency power, argon plasma flow of 8 L/min, auxiliary gas flow of 0.2 L/min, nebulizer gas flow of 0.5 L/min, axial plasma view and wavelength of 309.271 nm for Al^{3+}, 228.802 nm for Cd^{2+}, 221.648 nm for Ni^{2+} and 257.610 nm for Mn^{2+}. All the calibration solutions were prepared from a multi-element Al^{3+}, Cd^{2+}, Ni^{2+} and Mn^{2+} stock solution with a concentration of 1 g/L for each metal. All the samples were acidified with concentrated nitric acid (HNO_3, 69%) and filtered before being analyzed. The instrument response was periodically checked with the multi-element ICP QC standard solution (CHEM LAB) and with a blank (HNO_3, 5%).

Characterization of sorbents by Fourier transform infrared spectrometer, X-ray diffraction and scanning electron microscopy analysis

To identify the functional groups involved in the biosorption of DEK, Al^{3+}, Cd^{2+}, Ni^{2+} and Mn^{2+} by the sorbents, infrared spectra of the sorbents, with and without previous contact with the pollutants, were obtained using a Fourier transform infrared spectrometer (FTIR BOMEM MB 104). For the FTIR analyses, the sorbents were centrifuged and dried for 24 h at 60°C. Then, 10 mg of each sorbent was encapsulated in 100 mg of KBr (Riedel) in order to obtain a translucent sample disk. Background correction for atmospheric air was used for each spectrum. The resolution was 4 cm^{-1} and a minimum of 30 scans was conducted for each spectrum with a range between 500 and 4000 wavenumbers.

The X-ray diffraction (XRD) analyses were performed using a Philips PW1710 diffractometer. Scans were taken at room temperature in a 2θ range between 5° and 60°, using CuKα radiation.

Scanning electron microscopy (SEM) of the sorbents with and without previous contact with DEK, Al^{3+}, Cd^{2+}, Ni^{2+} and Mn^{2+} was performed on Leica Cambridge S360 to observe any morphological changes on the sorbents' surfaces.

Results and discussion

Lab-scale experiments – biosorption in batch systems

In these set of experiments, the initial concentration of DEK was kept constant (4 g/L), whereas the initial concentration of Al^{3+}, Cd^{2+}, Ni^{2+} and Mn^{2+} has increased from 5 to 100 mg/L. Percentages of DEK biodegradation and/or sorption higher than 95% were reached in 74 h, for the control containing just DEK and biomass. The same DEK removal percentage was achieved in solutions with initial concentrations of Al^{3+}, Cd^{2+}, Ni^{2+} and Mn^{2+} between 5 and 40 mg/L in 4 h and in 0.5 h, for initial concentrations of the same ions between 80 and 100 mg/L (Figure 1). These results suggest that, as the initial concentration of metals increases, the time required to achieve biodegradation and/or sorption percentages of DEK higher than 95% decreases significantly, meaning that the increase of the initial concentration of the metals accelerates the complete degradation and/or sorption of DEK. Complete biodegradation and/or sorption of DEK was obtained for the assays conducted with initial concentrations of metals equal to or higher than 20 mg/L. These results may be explained by the fact that the acclimation period obtained is shorter than the ones obtained with smaller concentrations of metal, and therefore the time required by the microbial culture to achieve the same level of performance is smaller [31]. The metabolites formed during the experiments (2-pentanone, methyl acetate, and ethyl acetate) were also completely biodegraded and/sorbed since at the end of the experiments they were not detected by GC-MS analysis. Studies conducted by Dilek et al. [32] and Gonzalez-Gil et al. [33] revealed that the presence on Ni^{2+} at low concentrations is not only nontoxic respectively to the microbial growth of the activated sludge and methanogenic sludge, but actually it enhances the microbial growth rate and metabolic activity. According to Nies [34], the majority of microorganisms overcome the presence of heavy metals (nonessential and essential metals, at low or high concentrations) by using two different mechanisms of metals' uptake. One of the mechanisms is essentially constitutively expressed and driven by the chemiosmotic gradient across the cytoplasmic membrane of the bacteria, being thus a fast and unspecified

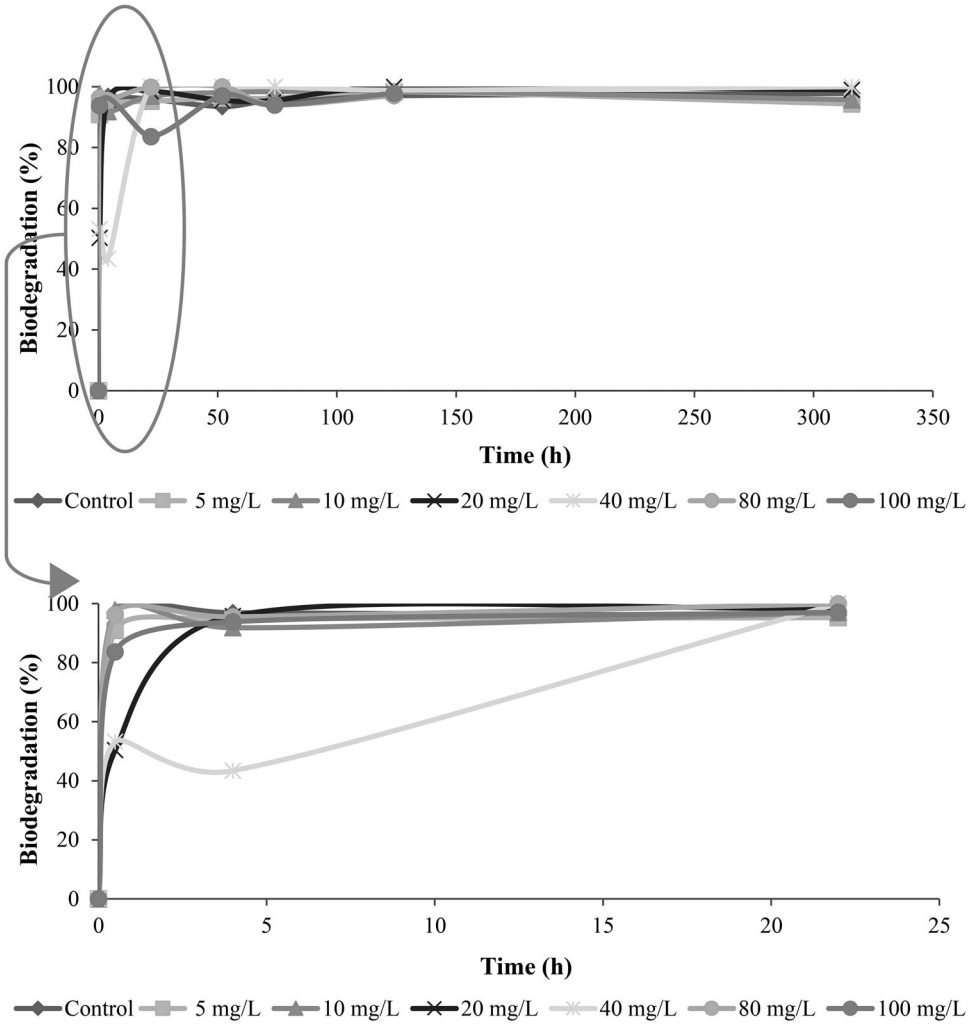

Figure 1. Biodegradation efficiency (%) of *S. equisimilis* for DEK (4 g/L) when exposed to different initial concentrations of metal ions, M.I., Al^{3+}, Cd^{2+}, Ni^{2+} and Mn^{2+} (5–100 mg/L).

mechanism. The other mechanism is used only by the microbial culture in specific circumstances (starvation or special metabolic conditions, for example), and uses adenosine triphosphate hydrolysis, as a way of obtaining energy. It is an inducible, very specific and slower mechanism than the first one described herein [35]. However, when exposed to high concentrations of metals (nonessential metals included), some microorganisms may develop a metal resistance mechanism, such as intra and extra-cellular sequestration, enzymatic detoxification, exclusion by permeability barrier and active transport efflux pumps, for example, allowing them not only to survive but also to grow in contaminated environments. It is important to highlight that to have a toxic or physiological effect, most metals have to enter the cell and to be present at high concentrations. The toxicity of nonessential heavy metals may occur through ligand interactions and/or through the displacement of the essential metals from their native binding sites. The toxicity effect itself (towards the microbial growth and towards the biodegradation of organic pollutant compounds) is dependent on the amount of metal bioavailable rather than the total or even soluble metal concentration present in the system [31].

The biosorption profiles of Al^{3+}, Cd^{2+}, Ni^{2+} and Mn^{2+} are quite different from each other (Figure 2) and from DEK. For initial concentrations of Al^{3+}, Cd^{2+}, Ni^{2+} and Mn^{2+} ranging between 5 and 80 mg/L, the biosorption efficiency (%) was found to follow the sequence $Al^{3+} > Cd^{2+} \geq Ni^{2+} \geq Mn^{2+}$, whereas for the experiments conducted with an initial concentration 100 mg/L of Al^{3+}, Cd^{2+}, Ni^{2+} and Mn^{2+} the biosorption efficiency (%) was found to follow the sequence $Al^{3+} > Ni^{2+} > Cd^{2+} > Mn^{2+}$. The affinity of microbial culture for a metal can be explained by the affinity between the metal cations and the negative charge of the cellular surface. Considering Pauling electronegativity, Ni (1.91 Pauling) has a higher electronegativity than Cd (1.69 Pauling), Al (1.61 Pauling) and Mn (1.55 Pauling). Despite their electronegativity and oxidation state, the reduced ionic radius of Al^{3+} and Ni^{2+} enhances their

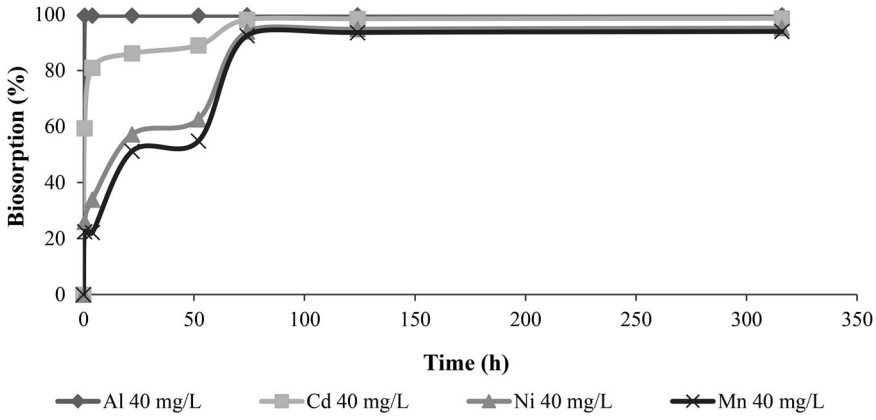

Figure 2. Biosorption efficiency (%) of *S. equisimilis* for Al^{3+}, Cd^{2+}, Ni^{2+} and Mn^{2+} (40 mg/L) when exposed to DEK (4 g/L).

penetration into the surface of the cell membrane, contributing thus to the overall results obtained. It is possible to observe that the essential metals (Ni^{2+}, Mn^{2+}) show lower biosorption performances, which, according to the literature, is unexpected. This behavior may be justified with the difference between the relative size of the ionic radius and the active sites of the biomass but also by the fact that many divalent heavy metal cations are structurally very similar, allowing the replacement of some essential cation metals for nonessential ones. In terms of uptake, with the exception of Al^{3+}, all the metals showed an increase in uptake with the increase in the initial concentration of each metal in the mixed solution and similar uptake profiles (Table 1). The results obtained with Al^{3+} could be explained by a reduced bioavailability of the metal in solution [31]. The use of mathematical models to describe the dynamics of the sorption processes is very important not only for the design of an operational control of the sorption process, but also because it is very helpful for the scale up and process optimization, allowing the description of the behavior of the sorption processes operating under different conditions.

Batch systems biodegradation and sorption kinetic modeling

The experimental results obtained for all the concentrations and for all the pollutants used in these assays were found to be best described by the pseudo-second-order kinetic model (Figure 3 and Table 2). For DEK, the K_2 constant increases with the increase in metal concentration, reaching its maximum value for 40 mg/L. For initial concentrations of metal higher than 40 mg/L, the K_2 constant starts to decrease, suggesting that for the range of metals with an initial concentration between 5 and 40 mg/L inclusive, the biodegradation and/or sorption rate of DEK by *S. equisimilis* increases over time, whereas for higher initial concentration of metal it decreases. This behavior may be explained by the saturation of the active sites on the biomass surface, as well as by the development of an inhibitory effect on the cellular growth. For aluminum, the K_2 constant increased with the increase in initial metal concentration, until an initial concentration of 80 mg/L was used, indicating that the biosorption rate increases through time. For initial concentrations higher than 80 mg/L, the K_2 constant decreases, revealing that for initial concentrations higher than 80 mg/L, the biosorption rate decreases. For cadmium, the K_2 constant decreases with the increase in metal concentration, until a maximum value of 80 mg/L. These results suggest that for the range of metals with an initial concentration between 5 and 80 mg/L inclusive, the sorption rate of Cd^{2+} by *S. equisimilis* decreases over time. For nickel and manganese, the K_2 constant decreases with the increase of metal concentration, suggesting that, as the initial concentration of metals increase, the sorption rate of Ni^{2+} and Mn^{2+} by

Table 1. Maximum and minimum uptake for different initial concentrations of Al^{3+}, Cd^{2+}, Ni^{2+} and Mn^{2+} for the lab-scale experiments.

Metal concentration (mg/L)		5	10	20	40	80	100
Al^{3+}	Time (h)	0.74	0.50	0.74	316	124	22
	Maximum uptake (mg/g)	0.97	0.96	0.95	0.96	0.98	0.96
Cd^{2+}	Time (h)	124	52	74	74	316	316
	Maximum uptake (mg/g)	1.62	3.2	6.39	13.15	26.24	32.77
Ni^{2+}	Time (h)	22	52	74	74	74	316
	Maximum uptake (mg/g)	1.59	3.23	6.32	12.97	25.86	31.79
Mn^{2+}	Time (h)	74	52	74	74	316	316
	Maximum uptake (mg/g)	1.58	3.19	6.24	12.53	25.74	31.39

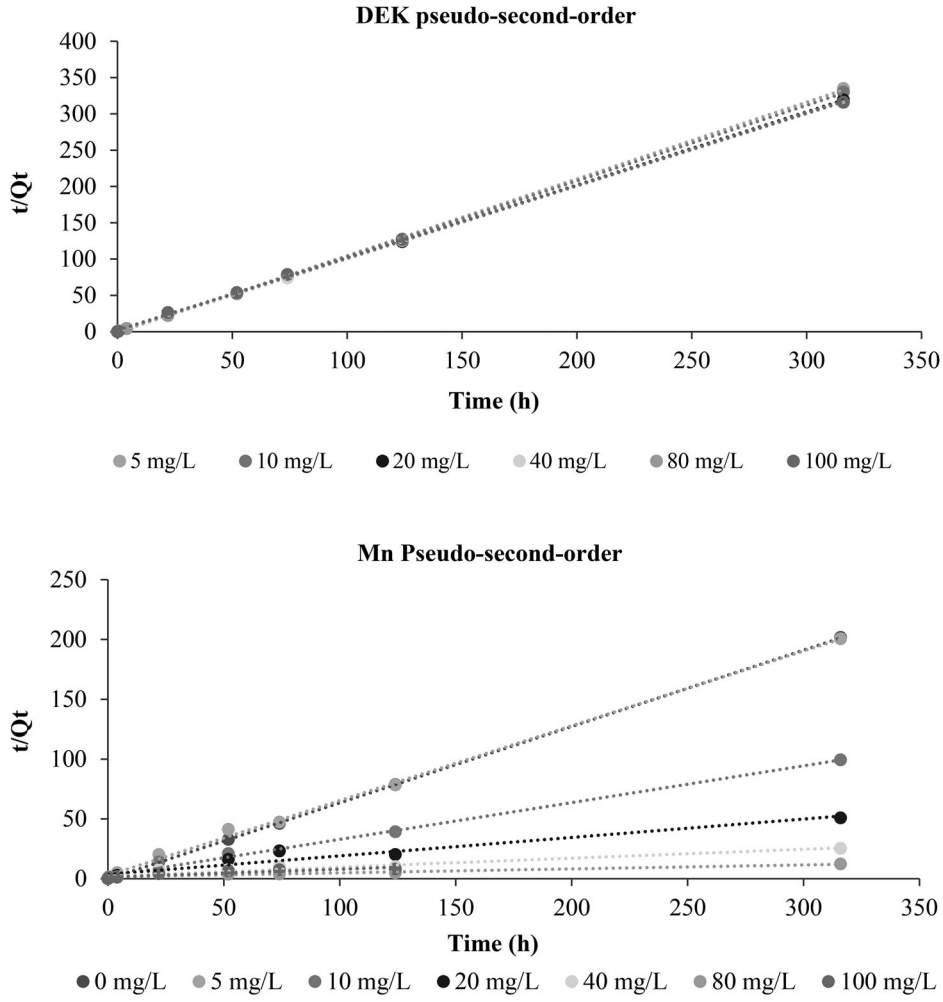

Figure 3. Kinetics model for DEK (DEK) and manganese (Mn) for the biosorption experiments conducted at lab-scale with *S. equisimilis*, when exposed to DEK (4 g/L) and Al^{3+}, Cd^{2+}, Ni^{2+} and Mn^{2+} (5–100 mg/L).

S. equisimilis decreases over time. These results can be justified by the saturation of the active sites on the cell surface, by the competition between the different metals and by their bioavailability to the microbial culture.

Viability tests were conducted at the end of the experiments and showed that the metabolic activity of *S. equisimilis* was adversely affected, since the number of colonies obtained were very small and only after several inoculations, the microbial growth presented a profile similar to the one obtained without the addition of DEK, Al^{3+}, Cd^{2+}, Ni^{2+} and Mn^{2+} in the culture medium. During all the experiments, the pH ranged between 4 and 4.5.

Pilot-scale experiments – biosorption studies in open systems

Pilot-scale experiments were conducted in a bioreactor column with a work solution volume of 40 L, with an initial concentration of DEK of 7.5 g/L, 100 mg/L of Al^{3+}, Cd^{2+}, Ni^{2+} and Mn^{2+} and 700 g of vermiculite. As previously mentioned, DEK was added to the working solution at different times, in order to continuously supply a carbon source to the system and also to infer about its impact on the metal sorption. It was found that for all the pollutants studied, the sorption percentage tends to increase through time and it follows the sorption order: DEK > Al^{3+} > Cd^{2+} ≈ Ni^{2+} > Mn^{2+} (Table 3). The results obtained for Al^{3+} can be justified by the small ionic radius (0.50 Å) that facilitates its sorption by the cell surface and its penetration into the intracellular space. The results obtained for Cd^{2+} and Ni^{2+} are very similar, which is unexpected since Ni has a smaller ionic radius (0.78 Å) and a higher electronegativity (1.91 Pauling) than Cd (0.97 Å, 1.69 Pauling). These results may be explained by their bioavailability and structural similarity that can trigger the substitution of Ni^{2+} uptake by Cd^{2+} by the cell enzymes. The reduced sorption obtained for Mn^{2+} may be due to

Table 2. Fitting parameters for pseudo-second-order kinetic model obtained for DEK, Al^{3+}, Cd^{2+}, Ni^{2+} and Mn^{2+} for the lab-scale experiments.

		Pseudo-second-order	
System	Pollutant	K_2	R^2
Control	DEK	4.009	0.999
	Al^{3+}	−4.320	0.999
	Cd^{2+}	1.598	1
	Ni^{2+}	−1.390	1
	Mn^{2+}	−1.587	1
S. equisimilis, 4 g/L DEK, 5 mg/L Al^{3+}, Cd^{2+}, Ni^{2+}, Mn^2	DEK	1.361	0.999
	Al^{3+}	28.952	1
	Cd^{2+}	0.219	0.999
	Ni^{2+}	0.204	1
	Mn^{2+}	0.138	0.998
S. equisimilis, 4 g/L DEK, 10 mg/L Al^{3+}, Cd^{2+}, Ni^{2+}, Mn^2	DEK	1.406	0.999
	Al^{3+}	78.588	1
	Cd^{2+}	0.088	0.999
	Ni^{2+}	0.052	0.999
	Mn^{2+}	0.043	0.994
S. equisimilis, 4 g/L DEK, 20 mg/L Al^{3+}, Cd^{2+}, Ni^{2+}, Mn^2	DEK	2.747	0.999
	Al^{3+}	51.637	1
	Cd^{2+}	0.016	0.993
	Ni^{2+}	0.006	0.937
	Mn^{2+}	0.006	0.940
S. equisimilis, 4 g/L DEK, 40 mg/L Al^{3+}, Cd^{2+}, Ni^{2+}, Mn^2	DEK	5.215	1
	Al^{3+}	111.813	1
	Cd^{2+}	0.018	0.999
	Ni^{2+}	0.004	0.972
	Mn^{2+}	0.002	0.930
S. equisimilis, 4 g/L DEK, 80 mg/L Al^{3+}, Cd^{2+}, Ni^{2+}, Mn^2	DEK	1.110	0.999
	Al^{3+}	190.001	1
	Cd^{2+}	0.003	0.994
	Ni^{2+}	0.002	0.984
	Mn^{2+}	0.001	0.903
S. equisimilis, 4 g/L DEK, 100 mg/L Al^{3+}, Cd^{2+}, Ni^{2+}, Mn^2	DEK	0.450	0.999
	Al^{3+}	116.40	1
	Cd^{2+}	0.299	0.748
	Ni^{2+}	0.001	0.976
	Mn^{2+}	0.003	0.840

the ionic radius of Mn^{2+} (0.80 Å) combined with its reduced electronegativity (1.55 Pauling), considering the small porosity of vermiculite. It was also observed that the complete sorption and/or biodegradation of DEK (as well as its metabolites – 2-pentanone, methyl acetate and ethyl acetate) was reached and that after each addition of DEK to the system, the sorption of each metal gradually increased (Figure 4). This behavior may be explained by a state of carbon depletion, which, after being overcome, led to a positive stimulus not only for the development of the biofilm but also for the decontamination of the mixed solution. The time required to achieve sorption and/or biodegradation percentages of DEK equal to or higher than 95% was higher than in the lab-scale experiments (168, 192 and 408 h). This can be justified by the increase in the acclimation period, by the open system operation with continuous feeding, and by the formation of non-specific metallic complex compounds within the cell, that increase their toxic and inhibitory effects, thus affecting the overall bacterial metabolism. During the pilot-scale experiments the pH ranged between 4 and 5.

Table 3. Biosorption performance of the bioreactor column for DEK (7.5 g/L) and for Al^{3+}, Cd^{2+}, Ni^{2+} and Mn^{2+} (100 mg/L).

	Biosorption efficiency (%)				
Time (h)	DEK	Al^{3+}	Cd^{2+}	Ni^{2+}	Mn^{2+}
First period – 528 h	93.04	99.47	16.93	31.75	26.68
Second period – 1992 h	100	98.85	36.88	44.43	47.81
Third period – 2928 h	100	99.85	41.75	49.03	52.03

Viability tests were conducted at the end of the experiments and revealed that the *S. equisimilis* biofilm presented a normal biological activity after the first inoculation. *S. equisimilis* in the form of biofilm seems to be more resistant to the toxic effects of high concentrations of Al^{3+}, Cd^{2+}, Ni^{2+} and Mn^{2+}, when compared to the bacteria in suspension (lab-scale experiments – biosorption in batch systems section). These results are in agreement with the literature, since the biofilm community offers several benefits such as easy access to substrate [36], protection against hazardous compounds due to the polymeric matrix that compose the biofilm and that acts as a diffusion barrier, increasing the resistance of the cells against toxic substances and/or environmental conditions [37].

Breakthrough curves modeling

Breakthrough curves are essential for industrial application of biosorption and/or biodegradation process since they provide essential information regarding the behavior of a column sorption process in the treatment of solutions of hazardous pollutants. The breakthrough point is defined as the pre-established saturation concentration accepted for the outflow of the system. Three breakthrough modeling equations have been tested in the present study: Adams-Bohart, Wolborska and Yoon and Nelson models. The Adam-Bohart and Wolborska models were applied to the experimental results in order to obtain a description of the initial part of the breakthrough curve. This approach was focused on the estimation of characteristic parameters such as the kinetic constant (k_{AB}) and the maximum absorption capacity (N_0) of the Adam-Bohart model and the kinetic coefficient of the external mass transfer (β_a) of the Wolborska model. The values of N_0, k_{AB} and β_a were calculated from the ln (C/C_0) versus t plot. In short fixed-bed column systems or in fixed-bed column systems with high flow rates, the axial diffusion is negligible, therefore if $k_{AB} \approx \beta_a/N_0$ and the Wolborska model approaches the Adams-Bohart model. The Yoon and Nelson model was used to investigate the breakthrough behavior of the pollutants with the *S. equisimilis* biofilm in a column bioreactor. The value of k_{YN} and τ were determined from the ln [$(C/(C_0 - C)$]

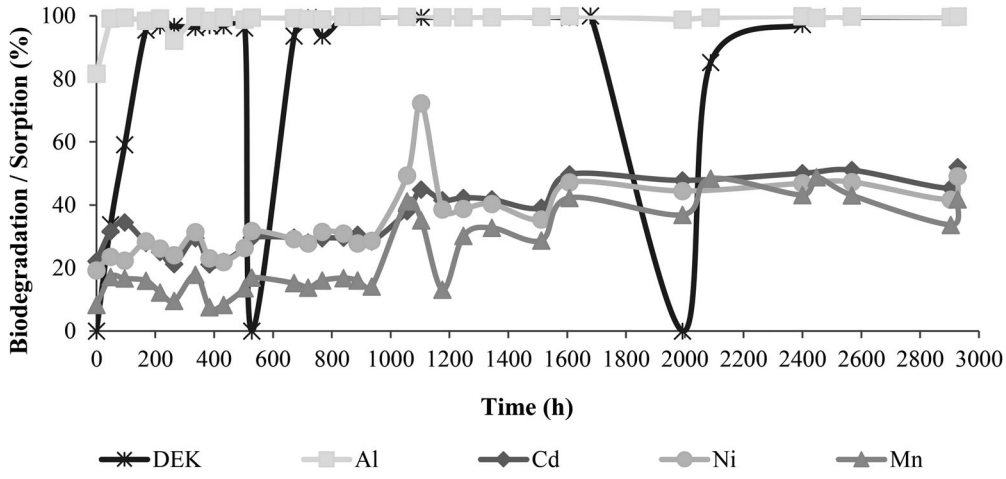

Figure 4. Sorption performance (%) of *S. equisimilis* biofilm supported on vermiculite for DEK (7.5 g/L) when exposed to initial concentrations of 100 mg/L of Al^{3+}, Cd^{2+}, Ni^{2+} and Mn^{2+}.

versus *t* plot. Predicted and experimental breakthrough curves are shown in Figure 5 and all the calculated parameters are presented in Table 4. A linear relationship between ln (C/C_0) and *t* was obtained for all the breakthrough curves (data concerning Al^{3+} were not considered) for all the periods of time considered and for all the breakthrough curves. The results obtained for DEK and for Al^{3+} are not properly described by any of the models employed ($R^2 < 0.750$, data not shown). Figure 5(a) and 5(b) shows that the Adams-Bohart and Wolborska model are a good fit to describe the breakthrough curve obtained for Cd^{2+} ($R^2 > 0.889$), which was expected since the condition $k_{AB} \approx \beta_a/N_0$ is verified. The experimental results obtained for Mn^{2+} are best fitted by the Wolborska model ($R^2 > 0.867$). The kinetic coefficient of the external mass transfer (β_a) and the maximum sorption capacity (N_0) were found to be $3.63e^{-5}$ (h^{-1}) and $1.16e^{5}$ (mg/L), respectively. From Table 4 and Figure 5(c), it is possible to conclude that the experimental results obtained for Ni^{2+} are best described by the Yoon and Nelson model ($R^2 > 0.870$) and that the time required for 50% sorbate breakthrough is 2177 h. The remaining predicted τ values were found to be very similar to the experimental values (2400 h for Cd^{2+} and 2088 h for Mn^{2+}). So, it is therefore possible to infer that (i) Cd^{2+} equilibrium is not instantaneous; consequently the rate of the sorption is proportional to the residual capacity of the sorbent and to the concentration of the sorbing species and that the Wolborska model is equivalent to the Adams-Bohart model, (ii) Ni^{2+} sorption is favored in relation to the other metals (higher values obtained for N_0) and that the rate of decrease in the probability of sorption of each sorbate molecule is proportional to the probability of the sorbate sorption and the probability of sorbate breakthrough and (iii) Mn^{2+} presented a kinetic coefficient of the external mass transfer of $363e^{-3}$ h^{-1}. Once again, it is important to emphasize the combining action of different biological processes: (i) biodegradation processes (confirmed by the appearance of several metabolites during the experiments and by biosorption processes for DEK) and (ii) biosorption (influenced by several parameters such as ionic radius and Pauling electronegativity and through bioaccumulation processes or the four metals). For example, nickel and manganese can be bioaccumulated by the cells, being used afterwards by cell enzymes in metabolic processes.

FTIR, XRD and SEM analysis

FTIR spectra of unloaded and loaded vermiculite with DEK, and of *S. equisimilis* biomass in suspension and supported, eventually loaded with DEK and Al^{3+}, Cd^{2+}, Ni^{2+} and Mn^{2+}, in the range of 500–4000 cm^{-1} were taken to confirm the presence of functional groups that are commonly responsible for the sorption processes and are presented in Figure 6(a). It is possible to observe that vermiculite exhibits a number of sorption peaks, reflecting the complex nature of the clays. For the unloaded vermiculite, the band at 1000 cm^{-1} represents the Si–O–Si stretching, whereas the band at 1635 cm^{-1} is for H–O–H in absorbed water bending [37] and the band at 3400 cm^{-1} represents the OH functional group stretching vibration. Some of these band signals were also detected by several other authors [38] on clays and were found to correspond to surface functional groups responsible for the sorption of toxic substances (Dǒ gan et al. [39]). These groups may interact with the different types of pollutants used in the present study. Samples of vermiculite exposed to DEK and samples of

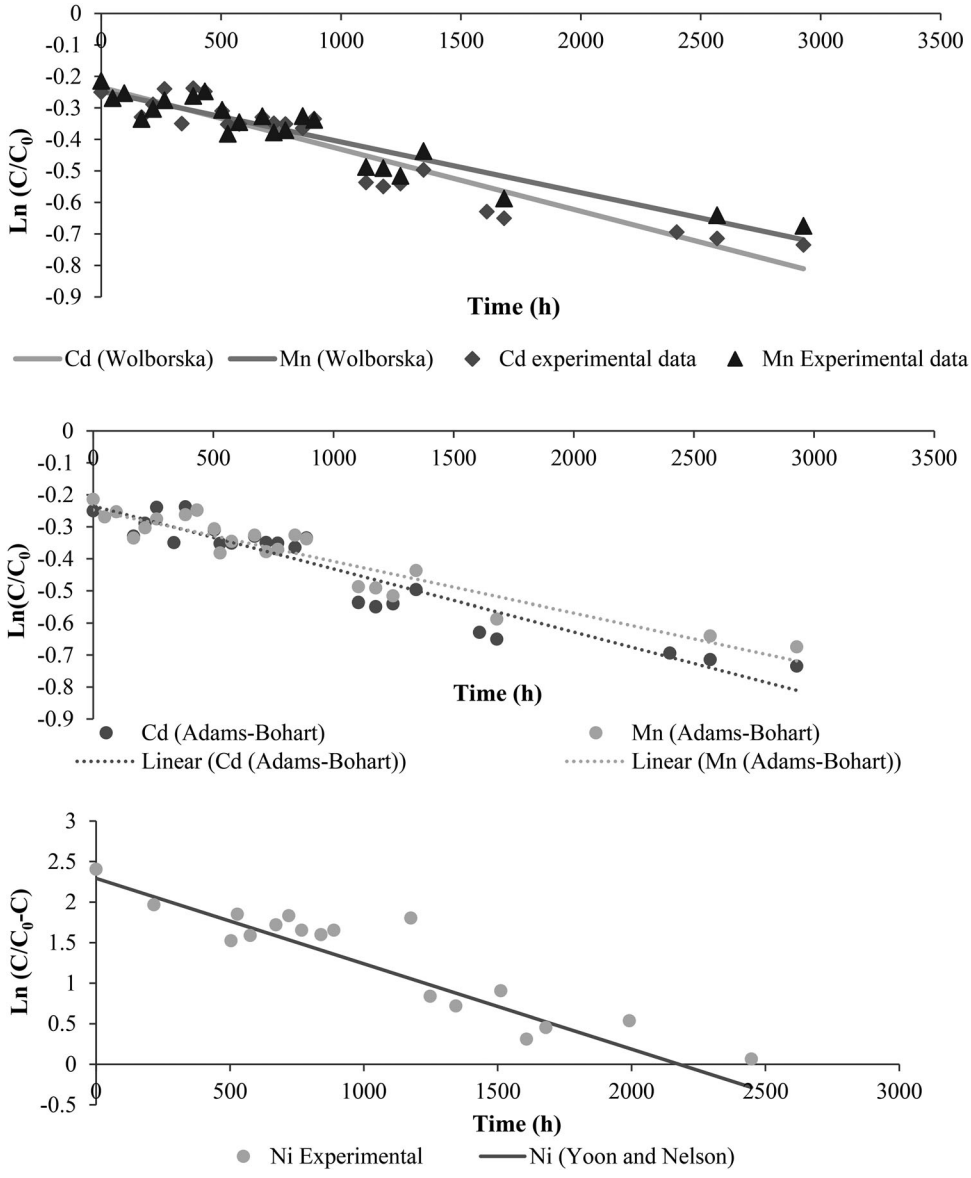

Figure 5. Predicted and experimental breakthrough curves for cadmium, manganese and nickel at pilot scale.

S. equisimilis biofilm supported into vermiculite and exposed to 7.5 g/L of DEK and 100 mg/L of Al^{3+}, Cd^{2+}, Ni^{2+} and Mn^{2+} reveal several changes on the intensity and/or on the shape of the peaks and the disappearance/formation of new peaks. After interaction with DEK, bands at 1400 cm^{-1} and at 2400 cm^{-1} corresponding respectively to C–H bending ($–CH_3$) and to C≡C and/or C≡N stretching, suffer significant changes, namely the first band, which disappeared and the second one presented higher intensity and different shape. For the bands detected at 675, 1000, 1650 and 3500 cm^{-1} and corresponding respectively to C–OH stretching vibrations, Si–O–Si stretching, C═O stretching groups and to the hydroxyl functional group stretching vibration (–OH), the intensity was found to decrease significantly. These changes may be due to the interaction and involvement of the functional groups present in the vermiculite surface with the functional groups of

Table 4. Breakthrough curves parameters obtained for the pilot-scale experiments.

	Adams-Bohart			Wolborska		Yoon and Nelson		
Pollutant	k_{AB} (L/mg h)	N_0 (mg/L)	R^2	β_a (h^{-1})	R^2	k_{YN} (h^{-1})	τ (h)	R^2
Cd^{2+}	$2.21e^{-5}$	−352194	0.895	$-6.17e^{-5}$	0.889	$-6.20e^{-4}$	2102	0.866
Ni^{2+}	$1.04e^{-5}$	57671	0.902	$-1.51e^{-3}$	0.891	$-1.05e^{-3}$	2177	0.892
Mn^{2+}	$1.58e^{-5}$	−236951	0.868	$3.63e^{-3}$	0.884	-4.83^{-4}	2547	0.866

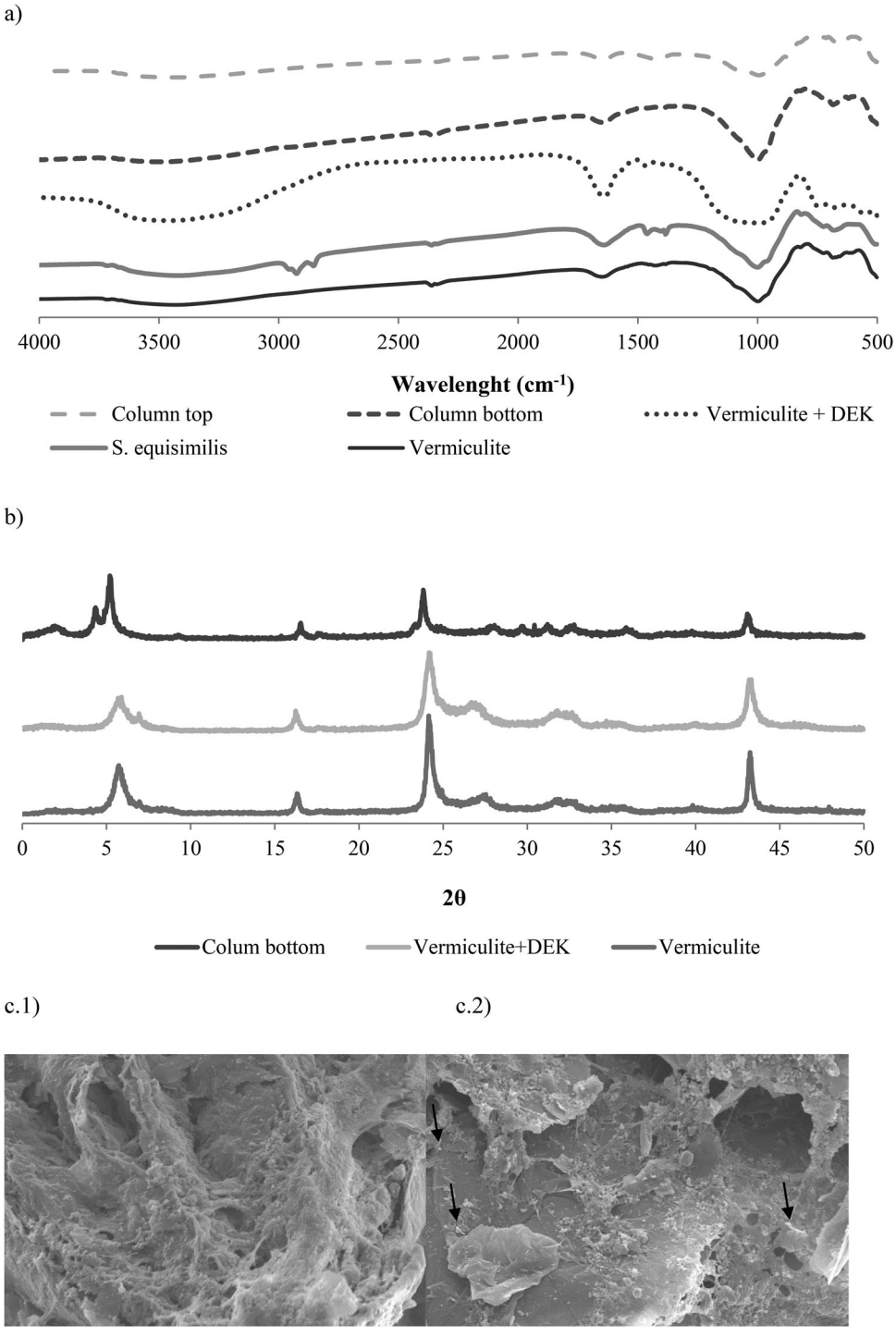

Figure 6. (a) FTIR spectra of different samples: vermiculite unloaded, *S. equisimilis* biomass, vermiculite loaded with DEK and *S. equisimilis* biofilm supported on vermiculite, loaded with DEK (7.5 g/L) and 100 mg/L of Al^{3+}, Cd^{2+}, Ni^{2+} and Mn^{2+} (at the bottom and at the top of the bioreactor column); (b) XRD patterns of original and recovered vermiculite; (c) SEM images of *S. equisimilis* supported on vermiculite (700 g) and exposed to DEK (7.5 g/L) and 100 mg/L of Al^{3+}, Cd^{2+}, Ni^{2+} and Mn^{2+} with an amplification of 1000× (c.1) at the middle of the bioreactor column and (c.2) at the bottom of the bioreactor column. The white incrustations correspond to the binding of metal ions on the surface of biomass and are an evidence of the biosorption of metal by the biofilm.

DEK, allowing its sorption by the clay. The samples of *S. equisimilis* biofilm supported into vermiculite and exposed to DEK and to the four metals reveal the disappearing of the bands at 2300 cm^{-1} and at 3500 cm^{-1}. For the sample collected at the top of the bioreactor column, the intensity of all peaks are significantly lower when compared to the peaks obtained only with vermiculite, whereas for the samples collected at the bottom of the

bioreactor column they presented peaks with higher intensity and with different shapes. These results may support the idea that the biomass present at the bottom of the column is exposed to higher concentrations of metals and DEK, whereas the biomass present at the top of the column is exposed to a lower concentration of these pollutants and therefore reduced toxicity, as the upwards circulation in the bioreactor leads to a higher sorption by the settled vermiculite and/or vermiculite biomass. These changes may be explained by the interaction of the functional groups of the different pollutants present in the solution. According to Volesky [40], the main functional groups responsible for sorption processes are the phosphodiester, phosphonate, sulfonate, imidazole, hydroxyl, amide, carboxyl and carbonyl groups. Some of these functional groups (phosphate bands at 1237 cm^{-1} and carbohydrate bands at 1070 cm^{-1} next to hydrocarbon sorption bands in the wavelength region between 3000 and 2800 cm^{-1}) [41] are known to be present on the *Streptococcus* sp. surface and to be responsible for the biosorption and biodegradation of toxic compounds such as DEK [42].

The powder XRD diffraction patterns of different samples (unloaded and loaded vermiculite with DEK, and *S. equisimilis* biomass in suspension and supported, eventually loaded with DEK and Al^{3+}, Cd^{2+}, Ni^{2+} and Mn^{2+}) were recorded at 2θ range between 5°C and 60°C and some representative patterns are presented in Figure 6(b). The sample of vermiculite (unloaded) and the sample of vermiculite loaded with DEK exhibited the typical pattern of clays, with no obvious change in the position of the diffraction lines for clays after contact with DEK and with *S. equisimilis* biomass, DEK and Al^{3+}, Cd^{2+}, Ni^{2+} and Mn^{2}, although some loss of the diffraction peaks are observed. This similarity between the diffractograms indicates a comparative crystallinity of vermiculite after the loading with DEK and that this process does not promote any significant structural modification in the clays. Nonetheless, the samples of vermiculite loaded with the *S. equisimilis* biomass, DEK and the four heavy metals present several changes not only on the position of the diffraction lines but also in their intensity. These changes are an evidence of the extensive damage on the vermiculite structure and were observable at SEM.

At the end of the experiment, the biofilm was analyzed by SEM and it was possible to confirm the presence of a well-developed biofilm (Figure 6(c)) and a more glazed, polished surface, with broken and worn leaves of vermiculite. Several white incrustations are observable on the surface (black arrows). According to Sharma et al. [43], these incrustations represent the binding of metal ions on the surface of biomass and are an evidence of the biosorption of metal by the biofilm. Similar evidences were found in previous works conducted by Quintelas et al. [44]. These results corroborate the sorption of metals and biodegradation/sorption of DEK by the joint-system used in this work.

Conclusion

It was demonstrated that *S. equisimilis* is able to efficiently biodegrade high concentrations of DEK in the presence of heavy metals ($Al^{3+} > Cd^{2+} > Ni^{2+} > Mn^{2+}$). At pilot scale it was found that the biodegradation of DEK was complete and that the metal uptake, with the exception of Al^{3+}, increase through time and with the renewing of the contaminated solutions. FTIR, SEM and XRD analyses allow us to confirm the sorption of metals and DEK by the biomass and/or vermiculite surface. These results prove the excellent capacity of this system to simultaneously treat solutions contaminated with ketone and heavy metals.

Disclosure statement

No potential conflict of interest was reported by the authors.

Funding

This study was supported by the Portuguese Fundação para a Ciência e a Tecnologia under the scope of the strategic funding of UID/BIO/04469/2013 unit and COMPETE 2020 (POCI-01-0145-FEDER-006684) and BioTecNorte operation (NORTE-01-0145-FEDER-000004) funded by European Regional Development Fund under the scope of Norte2020 – Programa Operacional Regional do Norte. Filomena Costa thanks FCT for a PhD Grant (SFRH/BD/77666/2011).

References

[1] Ogbodu RO, Omorogie MO, Unuabonah E, et al. Biosorption of heavy metals from aqueous solutions by Parkia biglobosa biomass: Equilibrium, kinetics, and thermodynamic studies. Environ Prog Sustain Energy. 2015;34:1694–1704.

[2] Ibrahim WM, Mutawie HH. Bioremoval of heavy metals from industrial effluent by fixed-bed column of red macroalgae. Toxicol Ind Health. 2013;29:38–42.

[3] Azeez L, Adeoye MD, Lawal AT, et al. Assessment of volatile organic compounds and heavy metals concentrations in some Nigerian-made cosmetics. Anal Chem: Indian J. 2013;12:443–483.

[4] Tam NFY, Wong YS, Wong MH. Effects of acidity on acute toxicity of aluminium-waste and aluminium-contaminated soil. Hydrobiology. 1989;188–189:385–395.

[5] Bennett BG. Environmental nickel pathways in man. In: F. W. Sunderman Jr, editor. Nickel in the human environment. Proceedings of a joint symposium, IARC scientific publication n°. 53. Lyon: International Agency for Research on Cancer; 1987. p. 487–495.
[6] Suazo-Madrid A, Morales-Barrera L, Aranda-Garcia E, et al. Nickel (II) biosorption by *Rhodotorula glutinis*. J Ind Microbiol Biotechnol. 2011;38:51–64.
[7] ATSDR. Toxicological profile for manganese. Atlanta, GA: US Department of Health and Human Services, Public Health Service, Agency for Toxic Substances and Disease Registry; 2000.
[8] ATSDR. Toxicological profile for aluminium. Atlanta, GA: US Department of Health and Human Services, Public Health Service, Agency for Toxic Substances and Disease Registry; 1992.
[9] Bondy SC. Low levels of aluminum can lead to behavioral and morphological changes associated with Alzheimer's disease and age-related neurodegeneration. Neurotoxicology. 2016;52:222–229.
[10] http://www.cadmium.org
[11] Ahmed S, Chughtai S, Keane MA. The removal of cadmium and lead from aqueous solution by ion exchange with Na-Y zeolites. Sep Purif Technol. 1998;13:57–64.
[12] http://pubchem.ncbi.nlm.nih.gov/
[13] http://toxnet.nlm.nih.gov/index.html
[14] Lam K-Y, Davidson FF, Hanson RK. High-temperature measurements of the reactions of OH with a series of ketones: acetone, 2-butanone, 3-pentanone, and 2-pentanone. J Phys Chem A. 2012;116:5549–5559.
[15] Quintelas C, Costa F, Tavares T. Bioremoval of diethylketone by the synergistic combination of microorganisms and clays: uptake, removal and kinetic studies. Environ Sci Pollut Res. 2012;2:1374–1383.
[16] www.cdc.gov
[17] Costa F, Quintelas C, Tavares T. Kinetics of biodegradation of diethylketone by arthrobacter viscosus. Biodegradation. 2012;23:81–92.
[18] Costa F, Neto M, Nicolau A, et al. Biodegradation of diethylketone by Penicillium sp. and Alternaria sp. – a comparative study. Curr Biochem Eng. 2015;2:81–89.
[19] Raulino GSC, Vidal CBV, Lima ACA, et al. Treatment influence on Green coconut shells for removal of metal ions: pilot-scale fixed-bed column. Environ Technol. 2014;35:1711–1720.
[20] Raghuvanshi S, Babu BV. Biofiltration for removal of methyl isobutyl ketone (MIBK): experimental studies and kinetic modelling. Environ Technol. 2010;31:29–40.
[21] Dobson RS, Burgess JE. Biological treatment of precious metal refinery wastewater: a review. Miner Eng. 2007;20:519–532.
[22] Amor L, Kennes C, Veiga MC. Kinetics of inhibition in the biodegradation of monoaromatic hydrocarbons in presence of heavy metals. Bioresour Technol. 2001;78:181–185.
[23] Kishore G, Sree P, Krishna D. Industrial wastes as adsorbents for the removal of chromium from waste water: a review. Int J Chem Sci. 2013;11:1371–1384.
[24] Awwad AM, Salem NM. Kinetics and thermodynamics of Cd(II) biosorption onto loquat (*Eriobotrya japonica*) leaves. J Saudi Chem Soc. 2014;18:486–493.
[25] Ghosh P, Thakur IS. Biosorption of landfill leachate by Phanerochaete sp. ISTL01: isotherms, kinetics and toxicological assessment. Environ Technol. 2016. http://dx.doi.org/10.1080/09593330.2016.1244218
[26] Yoon YH, Nelson JH. Application of gas adsorption kinetics. I. A theoretical model for respirator cartridge service life. Am Ind Hyg Assoc J. 1984;45:509–516.
[27] Wolborska A. Adsorption on activated carbon of p-nitrophenol from aqueous solution. Water Res. 1989;23:85–91.
[28] Bohart GS, Adams EQ. Some aspects of the behaviour of charcoal with respect to chlorine. J Am Chem Soc. 1920;42:523–544.
[29] Al-Haj-Ali A, Al-Hunaidi T. Breakthrough curves and column design parameters for sorption of lead ions by natural zeolite. Environ Technol. 2004;25:1009–1019.
[30] Wolborska A, Pustelnik P. A simplified method for determination of the break-through time of an adsorbent layer. Water Res. 1996;30:2643–2650.
[31] Olaniran AO, Balgobind A, Pillay B. Bioavailability of heavy metals in soil: impact on microbial biodegradation of organic compounds and possible improvement strategies. Int J Mol Sci. 2013;14:10197–10228.
[32] Dilek FB, Gokcay CF, Yetis U. Combined effects of Ni(II) and Cr(VI) on activated sludge. Water Res. 1998;32:303–312.
[33] Gonzalez-Gil G, Kleerebezem R, Lettinga G. Effects of nickel and cobalt on kinetics of methanol conversion by methanogenic sludge as assessed by on-line CH_4 monitoring. Appl Environ Microbiol. 1999;65:1789–1793.
[34] Nies DH. Microbial heavy metal resistance. Appl Environ Microbiol. 1999;51:730–750.
[35] Ji G, Silver S. Bacterial resistance mechanisms for heavy metals of environmental concern. J Ind Microbiol. 1995;14:61–75.
[36] Comte S, Guibaud G, Baudu M. Biosorption properties of extracellular polymeric substances (EPS) resulting from activated sludge according to their type: soluble or bound. Process Biochem. 2006;41:815–823.
[37] Covelo EF, Veja FA, Andrade ML. Competitive sorption and desorption of heavy metals by individual soil components. J Hazard Mater. 2007;140:308–315.
[38] Omoike A, Chorover J. Spectroscopy study of extracellular polymeric substances from *Bacillus subtillis*: aqueous chemistry and adsorption effects. Biomacromolecules. 2004;5:1219–1230.
[39] Dǒ gan M, Turhan Y, Alkan M, et al. Functionalized sepiolite for heavy metal ions adsorption. Desalination. 2008;230:248–268.
[40] Volesky B. Biosorption and me. Water Res. 2007;41:4017–4029.
[41] Van der Mei HC, Naumann D, Busscher HJ. Grouping of *Streptococcus mitis* strains grown on different growth media by FT-IR. Infrared Phys Technol. 1996;37:561–564.
[42] Costa F, Quintelas C, Tavares T. An approach to the metabolic degradation of diethylketone (DEK) by *Streptococcus equisimilis*: effect of DEK on the growth, biodegradation kinetics and efficiency. Ecol Eng. 2014;70:183–188.
[43] Sharma M, Kaushik A, Somvir BK, et al. Sequestration of chromium by exopolysaccharides of Nostoc and Gloeocapsa from dilute aqueous solutions. J Hazard Mater. 2008;157:315–318.
[44] Quintelas C, Figueiredo H, Tavares T. The effect of clay treatment on remediation of diethylketone contaminated wastewater: uptake, equilibrium and kinetics studies. J Hazard Mater. 2011;186:1241–1248.